Investigations of solid liquid interfaces in ultra-thin liquid films via single particle tracking of silica particles

Ines Trenkmann[1], *Daniela Täuber*[1], *Michael Bauer*[1], *Jörg Schuster*[1], *Sangho Bok*[2], *Shubhra Gangopadhyay*[2], *Christian von Borczyskowski*[1]

[1] Chemnitz University of Technology, Institute of Physics and nanoMA, Germany
[2] University of Missouri, Dept. of Electrical and Computer Engineering, USA

Corresponding author:
Ines Trenkmann
Institute of Physics
Chemnitz University of Technology
Reichenhainer Strasse 70
09126 Chemnitz
E-Mail: ines.trenkmann@s2003.tu-chemnitz.de

Abstract

Single particle tracking with a wide field microscope is used to study the solid liquid interface between the viscous liquid tetrakis(2-ethylhexoxy)-silane and a silicon dioxide surface. Silicon dioxide nanoparticles (5 nm diameter) marked with the fluorescent dye rhodamine 6G are used as probes. The distributions of diffusion coefficients, obtained by mean squared displacements, reveal heterogeneities with at least two underlying diffusion components. Measurements on films with varying film thicknesses show that the slower component is independent of the film thickness, while the faster one increases with the film thickness. Additionally, we could show that the diffusion behavior of the particles cannot be sufficiently described by only two diffusion coefficients.

keywords: diffusion, single particle tracking, squared displacements, msd, csdd, hydrodynamic boundary conditions, ultra-thin liquid films

1. Introduction

Single particle tracking (SPT) in living cells is one of the most commonly used techniques for real-time in-situ studies of dynamics on a molecular level. For this purpose, biological complexes are labeled with fluorophores. Since organic fluorophores suffer from photobleaching nanoparticles containing a bunch of fluorophores as a kind of reservoir are then an alternative tool. Therefore it is essential to characterize the principle diffusion behavior of such fluorophoric systems. But also in other fields of science such as chromatography and wetting it is mandatory to know how the diffusion of particles changes by the transition from bulk liquid to ultra-thin films.

In bulk liquids the diffusion coefficient of a spherical particle in a highly diluted solution is given by the Stokes-Einstein-relation

$$D_\infty = \frac{k_\mathrm{B}T}{3\pi\eta a}, \tag{1}$$

where T is the temperature, η the viscosity of the solvent, a the diameter of the particle and k_B the Boltzmann constant.

In ultra-thin liquid films the diffusion of a particle is influenced by the properties of the confining boundaries. The velocity of the liquid near a solid interface is equal to that of the solid. For investigations of ultra-thin films via wide field microscopy the solid boundary is formed by a stationary substrate. Consequently, also the velocity of the film is zero near the interface to the substrate. In continuum mechanics this hydrodynamic boundary condition is named non-slip boundary.

In contrast to this, the so-called slip boundary condition is valid on the free interface between liquid and ambient air. This means that the liquid near the free interface possesses the same velocity as the bulk. Due to this the diffusion of particles depends on the distances to both interfaces. The resulting diffusion coefficient can be calculated by

$$D = D_\infty \left[1 - \frac{9}{32}\frac{a}{z} + \frac{3}{16}\frac{a}{d-z} \right], \tag{2}$$

where d is the film thickness and z the distance between the center of the particle and the substrate surface [1,2].

An important characteristic of the diffusion process is the mean first passage time, which is the average time the observed particle needs for vertical diffusion through the investigated film. In our experiments the mean first passage time is much smaller than the used exposure time (in the range of ten milliseconds) due to the thickness of the investigated films which is in the range of a few molecular layers only. Consequently just an average diffusion coefficient can be observed, which is given by

$$D = \frac{1}{d-a}\int_{\frac{a}{2}}^{d-\frac{a}{2}} D_\infty \left[1 - \frac{9}{32}\frac{a}{z} + \frac{3}{16}\frac{a}{d-z} \right] \mathrm{d}z. \tag{3}$$

Beside these dynamic heterogeneities caused by the distances to the boundaries there are also static ones which influence the particle diffusion. E.g. functional groups on the substrate surface could be reasons for the in- or decrease of the observed diffusion coefficients of the particles [3,4].

2. Experimental Details and Evaluation Methods

In the experiment we investigated ultra-thin films of liquid tetrakis(2-ethylhexoxy)-silane (TEHOS, *ABCR GmbH & Co. KG*) on silicon wafers with a 100 nm thick thermally grown silicon dioxide layer (ZfM, Chemnitz University of Technology). To minimize the amount of contaminations the substrates were cleaned carefully. For this the

substrates were immersed into a piranha solution for about one hour at 70 °C and afterwards glowed in the flame of a propane burner.

As fluorescent tracers we used silicon dioxide nanoparticles with a diameter of 5 nm which are marked with rhodamine 6G molecules. The tracers were added to a solution of a few percent of TEHOS in n-hexane (*Aldrich*) in a single particle concentration. The deposition of the films was carried out by dipping the substrates into the TEHOS solution. After the dip coating process, a waiting time of 30 minutes is necessary for the complete evaporation of the solvent. The thicknesses of the resulting films were determined by ellipsometry [5]. Experiments have been carried out for 7 nm, 10 nm and 30 nm thick films.

Figure 1: Schematic drawing of the wide field setup.

For the investigations we used a home-built wide field microscope, schematically depicted in figure 1. The tracers were excited with the 476 nm line of an argon/krypton-ion laser (*Coherent*, Innova 70C). For this the laser beam was focused on the back-focal plane of 100x0.9 NA objective (*Zeiss,* Epiplan Neofluar). The emission light of the tracers was collected by the same objective and focused via lens (focal length 250 mm) onto a back-illuminated electron multiplying charge-coupled device (EMCCD) camera (*Andor,* iXon DU897, cooled down to -70 °C) in the frame-transfer mode, which was used as a photon detector. The fluorescence signal of the tracers is separated from backscattered excitation light using a dichroic beamsplitter and a long pass filter (502 nm).

The focal depth of the microscope is about 3 μm, which is much larger than the thickness of the investigated films. Therefore the observed motion of the tracers is a two-dimensional projection of the three-dimensional diffusion onto a plane parallel to the sample.

The recorded movies consist of 36000 or 45000 images at frame rates of 20 fps and 50 fps (50 ms and 20 ms per frame, including a read-out delay of 1.74 ms), respectively. The size of the images was 200 pixels x 200 pixels corresponding to an area of about 21 μm x 21 μm. The movies were analyzed semi-automatically by software, which is described in [6] and [7]. The tracers appear as diffraction-limited bright spots whose positions could be determined by the software. For that purpose a two-dimensional Gaussian function is fitted to the spots. With an average signal-to-noise ratio of about seven, the localization accuracy of 30 nm is higher than the diffraction limit. The detected spots are linked to trajectories.
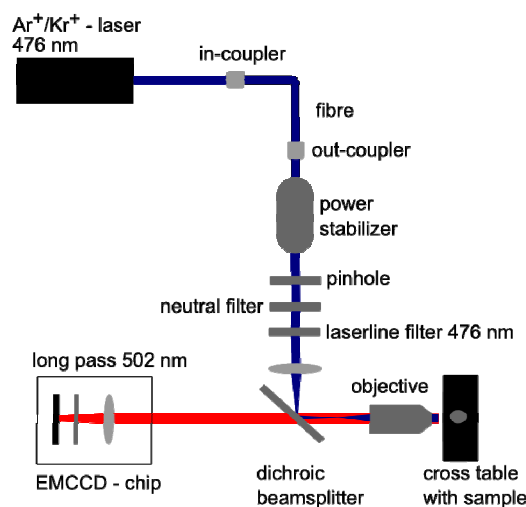
The obtained trajectories are analyzed in two different ways. In the first method a diffusion coefficient is calculated for each trajectory by a weighted linear fit of the determined mean squared displacement (msd)

$$\left\langle r^2(\tau) \right\rangle = \left\langle \left[r(\tau) - r(0) \right]^2 \right\rangle = 4D\tau \qquad (4)$$

along the trajectory [6]. All determined diffusion coefficients are plotted in histograms.

The msd yields accurate diffusion coefficients for homogeneous isotropic diffusion. In previous studies it could be shown that diffusion in ultra-thin films and nanopores is heterogeneous [5, 9 - 11]. Therefore the msd yields an average diffusion coefficient which depends on the underlying diffusion coefficients.

In a second method we calculated the squared displacements (sd) for the detected tracer positions between succeeding frames. From those sd the cumulative squared displacement distributions (csdd) were calculated as described recently [10]. These distributions represent the probability of finding a tracer outside a circle of the radius r after a time interval τ. In the following we rescaled the obtained squared displacements by dividing by

$$\frac{\mathsf{sd}}{4\tau} = di , \qquad (5)$$

where τ is the time between two succeeding frames and di is named diffusivity [11]. We chose the name diffusivity to make clear that by dividing the squared displacement with 4τ the resulting quantity is a short range diffusion coefficient between two succeeding frames whereas the diffusion coefficient D according to Stokes-Einstein denotes a macroscopic diffusion coefficient. The latter describes the long time diffusion behavior of the whole system, for which it is necessary to observe one single particle over a long period of time [12]. In contrast the distribution of diffusivities reveals the behavior within heterogeneous subsystems. Hence it is necessary to observe many particles over shorter times due to the stochastic character of the diffusion. As a result of the photobleaching of the fluorophores and their diffusion out of the recorded volume the observation time is limited. The evolution of squared displacements between succeeding frames offers the opportunity to use datasets of particles which are just visible for a few frames whereby the confidence level of the obtained mean diffusion coefficients is enlarged. As a result the mean diffusion coefficient could be determined from the diffusivities by

$$D = \lim_{n \to \infty} \frac{1}{n} \sum_{i=1}^{n} \frac{\mathsf{sd}_i}{4\tau} \qquad (6)$$

with n being the number of the gathered squared displacements.
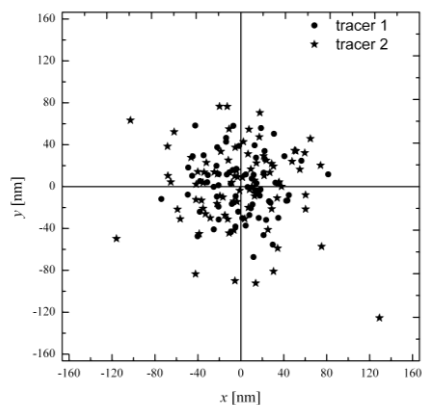
3. Results and Discussion

Figure 2: Scatter plot of the step size of two immobile tracers starting at the origin.
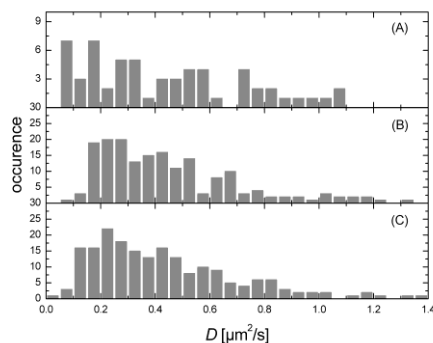

Figure 3: Distributions of the diffusion coefficients D for (A) 7 nm, (B) 10 nm and (C) 30 nm thick TEHOS films.

In all recorded frames mobile and immobile tracers could be observed. Detected trajectories of the latter were analyzed to assure that the investigated samples show no drift caused by external influences. For this purpose the step sizes of the trajectories were displayed as scatter plot starting at the origin. Two examples illustrated in figure 2 reveal that these tracers do not perform a directed motion. Furthermore, the determined msd show no time dependence. Hence it could be assumed that the diffusion of the mobile tracer is caused by Brownian motion.

For investigation of the influence of the film thickness on the diffusion coefficient three films with thickness 7 nm, 10 nm and 30 nm were analyzed. Figure 3 shows the distributions of the diffusion coefficients obtained by msd for all three film thicknesses. Therefore over 400 individual trajectories were analyzed. They consist of at least 50 frames (corresponding to an observation time of at least 2.5 s) and exceed an area of 1.1 μm^2. This selection criterion is necessary to avoid identifying immobile tracers with an apparent motion as mobile tracers. All three distributions show a broad range of diffusion coefficients from 0.025 μm^2/s to 1.4 μm^2/s. The analysis of single trajectories reveals that the diffusion of the tracers is inhomogeneous as has been shown in previous studies in our group on single Rhodamine 6G molecules in ultra-thin TEHOS films [9]. Beside periods which can be characterized by different coefficients we could frequently monitor periods in which the mobile tracers attach to the surface. It was not possible to clarify whether the tracers are adsorbed on the surface or trapped in a small region [13]. Through averaging along the trajectories these periods influence the apparent diffusion coefficients. We find that the distributions show no clear influence of the film thickness on the diffusion coefficients.

Therefore, in a second step we calculated the squared displacements and rescaled them using equation 5. The so obtained cumulative distributions are depicted in figure 4. For homogeneous diffusion a straight line is expected in a semi-log plot of the cumulative
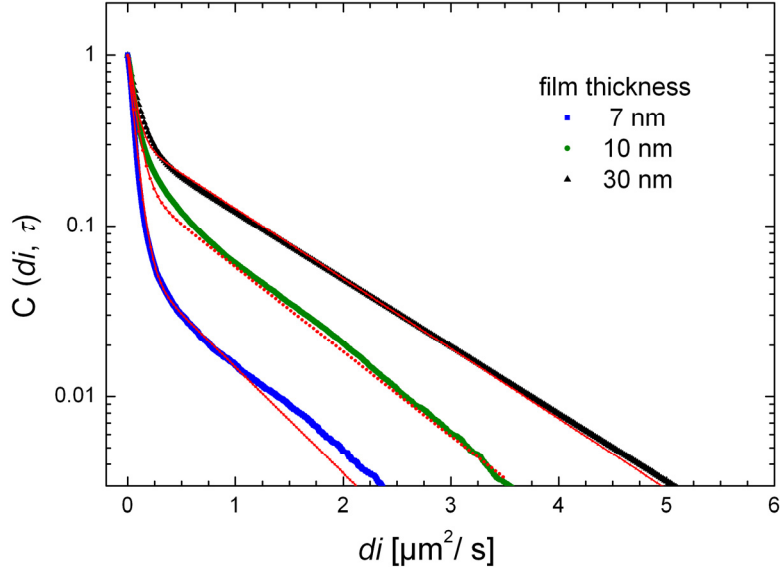
Figure 4: Cumulative distributions of diffusivities as a function of the film thickness, which were calculated by rescaling the obtained squared displacements using equation 5. The red curves (thin lines) show the fits according to equation 7.

distribution versus diffusivity. Our experimentally obtained data, however, yield a bi-exponential dependency of the form

$$\mathrm{C}(di, \tau) = \mathrm{A}_1 \exp\left(-\frac{di}{D_{\mathrm{slow}}}\right) + \mathrm{A}_2 \exp\left(-\frac{di}{D_{\mathrm{fast}}}\right), \tag{7}$$

where D_{slow} and D_{fast} are two mean diffusion coefficients corresponding to two subsystems. The obtained parameters are presented in table 1.

film thickness [nm]	A_1	D_{slow} [$\mu m^2/s$]	A_2	D_{fast} [$\mu m^2/s$]
7	(0.94 ± 0.01)	(0.06 ± 0.01)	(0.06 ± 0.02)	(0.71 ± 0.03)
10	(0.82 ± 0.03)	(0.07 ± 0.01)	(0.18 ± 0.04)	(0.87 ± 0.05)
30	(0.71 ± 0.02)	(0.06 ± 0.02)	(0.32 ± 0.03)	(1.05 ± 0.04)

Table 1: Diffusion components $D_{\mathrm{slow/fast}}$ and their fractions $\mathrm{A}_{1/2}$.

From this it follows that the observed diffusion depends at least on two diffusion mechanisms. The slow diffusion component D_{slow} remains constant within experimental accuracy by increasing the film thickness while the fast component D_{fast} depends on the film

thickness. We believe that the slow part D_{slow} of the distribution is caused by the diffusion along the substrate, e.g. by interaction of the tracers with silanol groups on the silicon dioxide surface [4].

To enable a comparison with the hydrodynamic boundary model we calculated the theoretically expected average diffusion coefficients. Therefore it is necessary to consider the influence of the applied video microscopy on the observed diffusion coefficients. Depending on the chosen exposure time t_{exp} and the time interval τ between two succeeding frames, which is given by the chosen number of recorded frames per second, the obtained diffusion coefficients are reduced by a factor c of

$$ c = 1 - \frac{2}{3}\frac{t_{exp}}{\tau} \tag{8} $$

according to [14]. Considering this influence in equation 3 the theoretically expected average diffusion coefficient is given by

$$ D = \left(1 - \frac{2}{3}\frac{t_{exp}}{\tau}\right)\frac{1}{d-a}\int_{\frac{a}{2}}^{d-\frac{a}{2}} D_\infty\left[1 - \frac{9}{32}\frac{a}{z} + \frac{3}{16}\frac{a}{d-z}\right]\mathrm{d}z \ . \tag{9} $$

The in this way calculated theoretical values and experimental determined values for the fast diffusion component D_{fast} are presented in table 2. The experimental values of D_{fast} are reduced by a factor of 8 compared to the theoretical ones. Nevertheless the relative changes between the different film thicknesses agree with the theoretical values. We want to outline one possible reason for the discrepancy between experiment and theory of the absolute values later on.

film thickness [nm]	experimental diffusion coefficient D_{fast} [$\mu m^2/s$]	theoretical diffusion coefficient D [$\mu m^2/s$]
7	0.7	6.0
10	0.9	7.9
30	1.1	8.4

Table 2: Experimentally obtained fast diffusion coefficients D_{fast} and calculated theoretical diffusion coefficients D (using equation 9).

We also observed a dependency of the determined diffusion coefficients on the sample age, similar to previous studies in our group on various dye molecules in ultra-thin TEHOS films [11, 15]. We investigated the diffusion behavior of the tracers in a 7 nm thick TEHOS film 1 h, 25 h and 49 h after preparation. Because the investigated system is a fluid, one would expect that the film thickness will decrease due to evaporation. Consequently the obtained diffusion coefficients will decrease with the film thickness. As a result of the low vapor pressure the TEHOS film evaporates with 1 nm
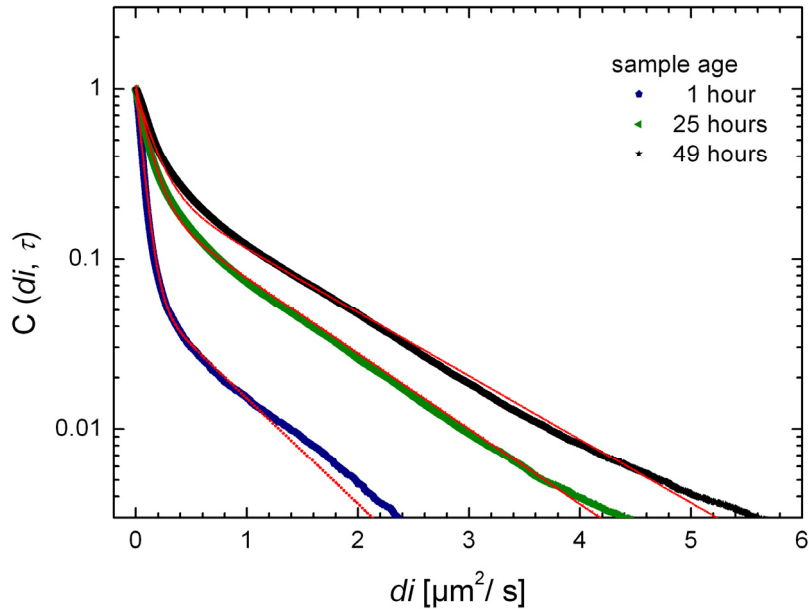
Figure 5: Cumulative distributions of diffusivities as a function of the sample age for a 7 nm thick TEHOS film. The red (thin) curves are bi-exponential fits given by equation 7.

per week [16]. Therefore we expect that the film thickness remains constant during that time and no change of the diffusion coefficients would be expected.

Sample age [h]	A_1	D_{slow} [$\mu m^2/s$]	A_2	D_{fast} [$\mu m^2/s$]
1	(0.94 ± 0.04)	(0.06 ± 0.01)	(0.06 ± 0.01)	(0.71 ± 0.03)
25	(0.83 ± 0.05)	(0.11 ± 0.01)	(0.21 ± 0.01)	(0.98 ± 0.07)
49	(0.72 ± 0.02)	(0.15 ± 0.01)	(0.27 ± 0.02)	(1.16 ± 0.05)

Table 3: Diffusion components $D_{slow/fast}$ and their fractions $A_{1/2}$

Figure 5 shows as a function of time the obtained cumulative distributions of the diffusivities. The curves were fitted to the bi-exponential function given in equation 7 and the obtained values are presented in table 3. Again we obtained two diffusion coefficients, a slow and a fast one which both increase with the sample age. The fraction A_1 of the slower diffusion component decreases while the fraction A_2 of the faster one increases. Assuming that the slow component is caused by diffusion along the surface of the substrate via interaction e.g. with silanol groups (jumping and sliding between hydrogen bonds [17]) an increase of the diffusion coefficient could be achieved by shielding the silanol groups [3]. This could be a result of a chemical reaction between
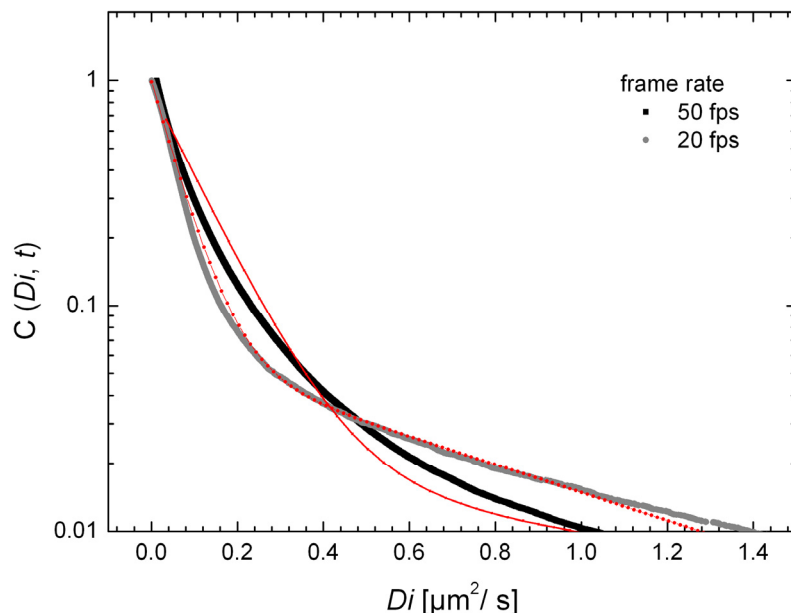
Figure 6: Cumulative distributions of diffusivities for a 7 nm thick TEHOS film obtained from frames recorded with 20 fps and 50 fps. The red (thin) curves are bi-exponential fits given by equation 7.

TEHOS molecules and water molecules adsorbed on the surface. But there is no finite answer for the observed increase of the fast diffusion component.

So far all shown results were obtained from frames which were recorded with 20 frames per second, which corresponds to a time interval of 50 ms between two succeeding frames. Additionally, for the 7 nm film we recorded frames with a time interval of $\tau = 20$ ms (corresponding to 50 fps).Because squared displacements depend on the time interval between two succeeding frames they will increase with decreasing frame rate. To enable a comparison of the obtained results of both chosen frame rates we removed the time dependency of the x-axis by rescaling the squared displacement using equation 5.

The obtained cumulative distributions of diffusivities are shown in figure 6. The curves for different frame rates clearly deviate from each other and therefore still show a time dependency. Both distributions were fitted with the bi-exponential function given in equation 7, and the obtained values are presented in table 4:

The data obtained with a frame rate of 50 fps yield increased values for both diffusion components. Additionally, the fraction of the fast component decreases in favor of the slow one.

frame rate [fps]	A_1	D_{slow} [$\mu m^2/s$]	A_2	D_{fast} [$\mu m^2/s$]
20	(0.94 ± 0.04)	(0.06 ± 0.01)	(0.06 ± 0.01)	(0.71 ± 0.03)
50	(0.96 ± 0.05)	(0.08 ± 0.02)	(0.04 ± 0.02)	(1.0 ± 0.2)

Table 4: Diffusion components $D_{slow/fast}$ and their fractions $A_{1/2}$

Like mentioned above we believe that the slow diffusion coefficient is caused by diffusion of the tracers along the silicon dioxide surface and the fast one by free diffusion in the film which is influenced by the hydrodynamic boundary conditions. Due to the small mean first passage time of the tracers compared to the exposure time we just observe an average diffusion coefficient. Therefore we model the investigated system as a two layer system, like depicted in figure 7. The first layer corresponds to the diffusion of the tracers along the surface, which is characterized by a diffusion coefficient D_1 and a dwell time τ_1 of the observed particles in this layer. The second layer corresponds to the free diffusion of the particles with an average diffusion coefficient D_2 and the dwell time τ_2. To observe the real diffusion coefficient for each layer it is necessary to use time intervals between succeeding frames which are smaller than the dwell times in each layer [18]. If the time interval between two recorded frames is longer than the dwell times in the specific layers the observed tracer will pass from one layer to the next one. This results in an average of both diffusion coefficients which depends on the dwell times in each layer [18].
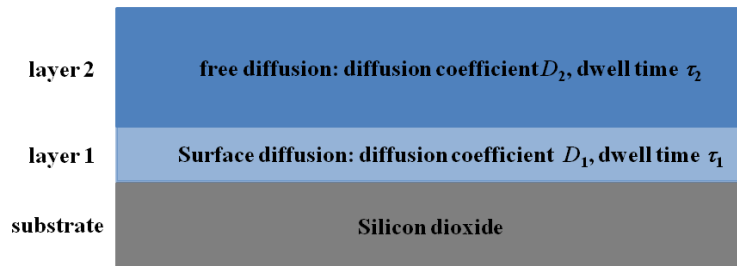

Figure 7: Schematic of the suggested two layer system

Therefore we suggested that the increase of the fast diffusion component between the two distributions depicted in figure 7 is caused by dwell times in the film which are smaller than the time intervals between two succeeding frames. Additionally, this explains why the obtained fraction of the fast diffusion coefficient is higher for the smaller frame rate.

Furthermore the short dwell times of tracers in layer 2 compared to the applied time interval explains the difference between the experimentally obtained values and the theoretically expected ones. Due to the long time interval compared to the short dwell time of the tracers in the free film we just observe an average diffusion coefficient which depends on the relation of the dwell time in the free film and the diffusion along the surface to the

time interval between two recorded frames. Therefore it is necessary to use time intervals which are smaller than the dwell times of the tracers in the film in order to enable the measurement of the actual diffusion coefficient in the free film.

4. Conclusion

In this paper we could show that the determination of diffusion coefficients by mean squared displacements is not a suitable tool for the analysis of the diffusion behavior in ultra-thin liquid films. Due to static and dynamic heterogeneities which lead to average diffusion coefficients the obtained distributions reveal no clear dependency on the film thickness. In contrast, the obtained cumulative distributions of diffusivities show two diffusion components. Thereby the slow diffusion coefficient remains constant and the faster one increases with the film thickness. Additionally the latter one shows the same relative changes with increasing film thickness as the values calculated via the hydrodynamic model. The difference between distributions obtained from recorded frames with different frames rates (corresponding to different time intervals between succeeding frames) could be caused by different dwell times in individual layers of the film. Due to dwell times which are much smaller than the chosen time intervals between succeeding frames it is only possible to obtain average diffusion coefficients. Measurements with even higher frame rates may allow to determine the actual underlying diffusion coefficients. Additionally, a comparison of these results with the obtained data of single dye molecules will be reported elsewhere [6, 11, 15].

References

[1]   E. Lauga, T. M. Squires, Phys. of Fluids 17 (2005) 103102.
[2]   B. Lin, J. Yu, S. A. Rice, Phys. Rev. E 62 (2000) 3909-3919.
[3]   T. Lebold, L. A. Mühlstein, J. Blechinger, M. Riederer, H. Amenitsch, R. Köhn, K. Peneva, K. Müllen, J. Michaelis, C. Bräuchle, T. Bein, Chemistry-A Eur. J. 15 (2009) 1661-1672.
[4]   A. Honciuc, D. K. Schwartz, JACS 131 (2009) 5973-5979.
[5]   J. Schuster, F. Cichos, C. von Borczyskowski, Eur. Polym. J. 40 (2004) 993-999.
[6]   J. Schuster, Dissertation, Chemnitz University of Technology, 2002.
[7]   M. Heidernätsch, master thesis, Chemnitz University of Technology, 2009.
[8]   M. J. Saxton, Biophys. J. 72 (1997) 1744-1753.
[9]   J. Schuster, F. Cichos, C. von Borczyskowski, Eur. Phys. J. E, 12 (2003) S75-S80.

[10] C. Hellriegel, J. Kirstein, C. Bräuchle, V. Latour, T. Pigot, R. Clivier, S. Lacombe, R. Brown, V. Guieu, C. Payrastre, A. Izquierdo, P. Mocho, J. Phys. Chem. B. 108 (2004) 14699-14709.

[11] D. Täuber, M. Heidernätsch, M. Bauer, G. Radons, J. Schuster, C. von Borczyskowski, Diffusion Fundamentals J. (2009) submitted.

[12] H. Qian, M. P. Sheetz, E. L. Elson, Biophys. J. 60 (1991) 910-021.

[13] C. Hellriegel, J. Kirstein, C. Bräuchle, New J. of Phys. 7 (2005) 23.

[14] D. Montiel, H. Cang, H. Yang, J. Phys. Chem. B 110 (2006) 19763.

[15] D. Täuber, unpublished results.

[16] M. L. Forcada, C. M. Mate, Nature, 363 (1993) 527-529.

[17] A. Honciuc, A. W. Harant, D. K. Schwartz, Langmuir 24 (2008) 6562-6566.

[18] M. Bauer, M. Heidernätsch, D. Täuber, C. von Borczyskowski, G. Radons, Diffusion Fundamentals J. (2009) submitted.